Article

Cell Reports

Central Insulin Action Activates Kupffer Cells by Suppressing Hepatic Vagal Activation via the Nicotinic Alpha 7 Acetylcholine Receptor

Graphical Abstract

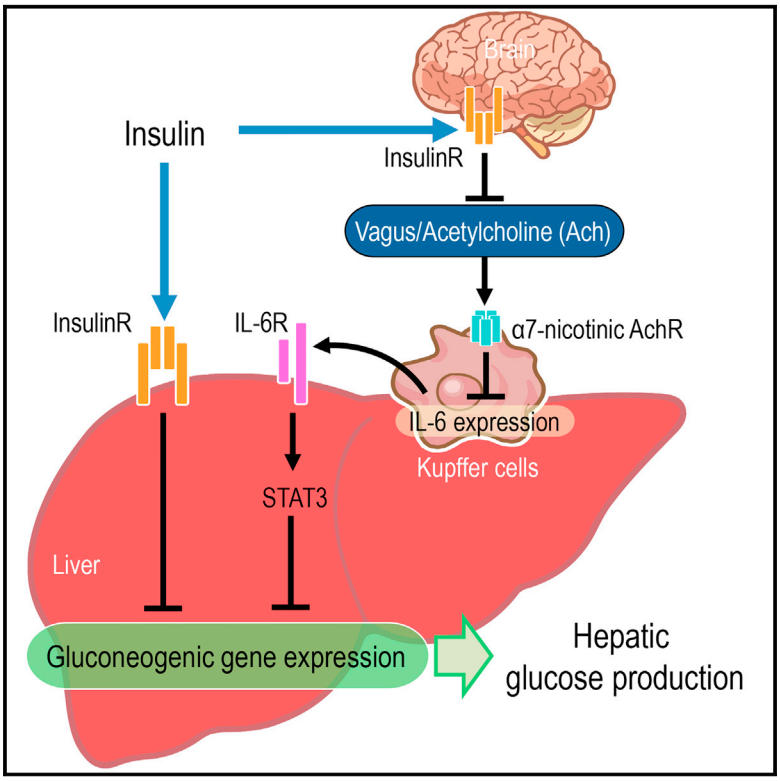

Authors

Kumi Kimura, Mamoru Tanida, Naoto Nagata, ..., Shuichi Kaneko, Masato Kasuga, Hiroshi Inoue

Correspondence

inoue-h@staff.kanazawa-u.ac.jp

In Brief

In this paper, Kimura et al. show a mechanism of the central insulin-mediated hepatic response, where central insulin action—known to suppress hepatic glucose production via hepatic IL-6/STAT3 activation—mitigates the α7-nAchR-dependent downregulation of IL-6 expression in Kupffer cells by the vagus nerve.

Highlights

- Central insulin action suppresses activity of the hepatic branches of the vagus nerve
- Central insulin action activates hepatic STAT3 by mitigating nAchR suppression
- α7-nAchR-mediated control of Kupffer cells is needed for the brain hepatic response
- Obesity impedes central insulin-dependent regulation of vagus nerve activity

Kimura et al., 2016, Cell Reports *14*, 2362–2374
March 15, 2016
http://dx.doi.org/10.1016/j.celrep.2016.02.032

OPEN ACCESS
CellPress

Cell Reports
Article

Central Insulin Action Activates Kupffer Cells by Suppressing Hepatic Vagal Activation via the Nicotinic Alpha 7 Acetylcholine Receptor

Kumi Kimura,[1,12] Mamoru Tanida,[2,12] Naoto Nagata,[3] Yuka Inaba,[1,4] Hitoshi Watanabe,[1] Mayumi Nagashimada,[3] Tsuguhito Ota,[3] Shun-ichiro Asahara,[5] Yoshiaki Kido,[5,6] Michihiro Matsumoto,[7] Koji Toshinai,[8,9] Masamitsu Nakazato,[8] Toshishige Shibamoto,[2] Shuichi Kaneko,[10] Masato Kasuga,[11] and Hiroshi Inoue[1,4,*]

[1]Department of Physiology and Metabolism, Brain/Liver Interface Medicine Research Center, Kanazawa University, Kanazawa, Ishikawa 920-8641, Japan
[2]Department of Physiology II, Kanazawa Medical University, Uchinada, Ishikawa 920-0293, Japan
[3]Department of Cell Metabolism and Nutrition, Brain/Liver Interface Medicine Research Center, Kanazawa University, Kanazawa, Ishikawa 920-8641, Japan
[4]Metabolism and Nutrition Research Unit, Institute for Frontier Science Initiative, Kanazawa University, Kanazawa, Ishikawa 920-8641, Japan
[5]Division of Diabetes and Endocrinology, Department of Internal Medicine, Kobe University Graduate School of Medicine, Kobe, Hyogo 650-0017, Japan
[6]Division of Medical Chemistry, Department of Biophysics, Kobe University Graduate School of Health Sciences, Kobe, Hyogo 654-0142, Japan
[7]Department of Molecular Metabolic Regulation, Diabetes Research Center, Research Institute, National Center for Global Health and Medicine, Tokyo 162-8655, Japan
[8]Department of Neurology, Respirology, Endocrinology, and Metabolism, Faculty of Internal Medicine, University of Miyazaki, Miyazaki, Miyazaki 889-1692, Japan
[9]Department of Sports and Fitness, Faculty of Wellness, Shigakkan University, Obu, Aichi 474-8651, Japan
[10]Department of Disease Control and Homeostasis, Graduate School of Medical Sciences, Kanazawa University, Kanazawa, Ishikawa 920-8641, Japan
[11]National Center for Global Health and Medicine, Tokyo 162-8655, Japan
[12]Co-first author
*Correspondence: inoue-h@staff.kanazawa-u.ac.jp
http://dx.doi.org/10.1016/j.celrep.2016.02.032

SUMMARY

Central insulin action activates hepatic IL-6/STAT3 signaling, which suppresses the gene expression of hepatic gluconeogenic enzymes. The vagus nerve plays an important role in this centrally mediated hepatic response; however, the precise mechanism underlying this brain-liver interaction is unclear. Here, we present our findings that the vagus nerve suppresses hepatic IL-6/STAT3 signaling via α7-nicotinic acetylcholine receptors (α7-nAchR) on Kupffer cells, and that central insulin action activates hepatic IL-6/STAT3 signaling by suppressing vagal activity. Indeed, central insulin-mediated hepatic IL-6/STAT3 activation and gluconeogenic gene suppression were impeded in mice with hepatic vagotomy, pharmacological cholinergic blockade, or α7-nAchR deficiency. In high-fat diet-induced obese and insulin-resistant mice, control of the vagus nerve by central insulin action was disturbed, inducing a persistent increase of inflammatory cytokines. These findings suggest that dysregulation of the α7-nAchR-mediated control of Kupffer cells by central insulin action may affect the pathogenesis of chronic hepatic inflammation in obesity.

INTRODUCTION

Insulin directly controls glucose metabolism in various target organs such as skeletal muscle, adipose tissue, and the liver, while also acting indirectly on the CNS to regulate glucose/energy metabolism (Plum et al., 2006; Schwartz et al., 2013). In fact, brain-specific insulin receptor knockout mice display insulin resistance, in addition to increased food intake, body weight, and obesity (Brüning et al., 2000). Various studies have indicated that central insulin action reduces hepatic glucose production (HGP), especially in rodents (Obici et al., 2002). Increased circulating levels of insulin result in the activation of hypothalamic insulin receptor/phosphatidylinositol 3-kinase (PI3-K) signaling, leading to the suppression of HGP via hypothalamic ATP-dependent potassium channels, which is activated by PI3-K (Carey et al., 2013; Prodi and Obici, 2006). Indeed, the suppression of HGP using the hyperinsulinemic-euglycemic clamp technique is impeded by insulin receptor deficiency, insulin receptor knockdown, and PI3-K inhibition in the hypothalamus (Inoue et al., 2006; Obici et al., 2002). Moreover, intracerebroventricular (ICV) administration of insulin and ATP-dependent potassium

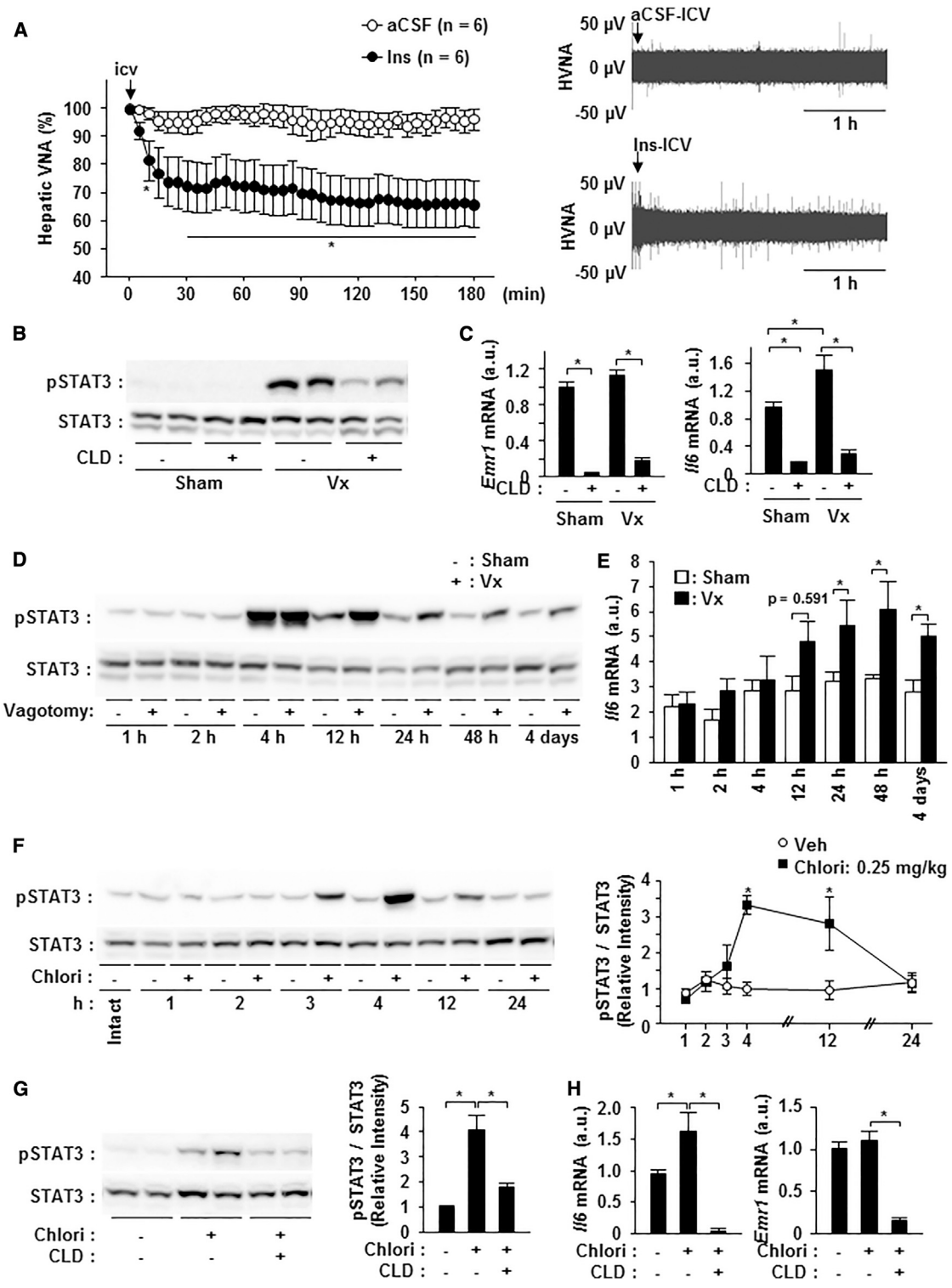

Figure 1. Central Insulin Action Suppresses Hepatic Vagal Activation, which Inhibits Hepatic IL-6/STAT3 Signaling

(A) Hepatic VNA after ICV insulin or artificial cerebrospinal fluid (aCSF) administration. The time-course changes in hepatic VNA after injection of aCSF or insulin are expressed as mean ± SE of the percentages of values at 0 min are shown on the left. The open circles are 2 μl of aCSF ICV bolus injection (n = 6). The closed circles are 40 μU/2 μl of insulin ICV bolus injection (n = 6) (significant differences between the aCSF group and insulin group from 30–180 min) ($p < 0.05$). A representative neurogram depicting the effect of ICV aCSF and insulin in mice is shown on the right.

(legend continued on next page)

channel activators reportedly reduce HGP (Obici et al., 2002; Pocai et al., 2005a). Several studies have revealed that ICV insulin-induced suppression of HGP is abolished by hepatic vagotomy, suggesting that central insulin action-induced hepatic responses are mediated by the vagus nerve (Pocai et al., 2005a, 2005b).

Central insulin action suppresses HGP by downregulating the gene expression of gluconeogenic enzymes such as *G6pc*, which encodes glucose-6-phosphatase (G6Pase). Previously, we reported the importance of hepatic IL-6/STAT3 signaling as an effector of the central insulin action-mediated hepatic response (Inoue et al., 2006). STAT3 is a ligand-dependent transcription factor that is phosphorylated via ligands such as interleukin-6 (IL-6) to become activated as a transcription factor (Akira, 1997). The expression of IL-6 in hepatic resident macrophages, Kupffer cells, increases following central insulin action, which leads to the paracrine activation of hepatocyte STAT3 and the subsequent suppression of gluconeogenic enzyme gene transcription (Inoue et al., 2004, 2006). It has also been reported that activated STAT3 binds to the promoter region of the *G6pc* gene to suppress its transcription (Ramadoss et al., 2009). Furthermore, hepatic STAT3 deficiency or systemic IL-6 deficiency results in insulin resistance and impaired suppression of HGP by ICV insulin, suggesting the importance of central insulin action-mediated hepatic IL-6/STAT3 signaling (Inoue et al., 2006). While the mechanism of insulin action in the CNS and the importance of hepatic IL-6/STAT3 signaling in the suppression of central insulin action-mediated HGP are being clarified, the mechanism of central insulin action-mediated control on the vagus nerve and hepatic IL-6/STAT3 signaling has not been elucidated fully.

The vagus nerve is known to perform crucial functions in modulating inflammation (Borovikova et al., 2000). In particular, electrical stimulation of the vagus nerve reportedly suppresses the induction of inflammatory cytokine expression including IL-6 in the liver following lipopolysaccharide (LPS) administration (Borovikova et al., 2000). Acetylcholine, which is the main neurotransmitter in the vagus nerve, reportedly suppresses the secretion of IL-6 via the α7-nicotinic acetylcholine receptor (α7-nAchR) in peritoneal macrophages (Wang et al., 2003). Indeed, the administration of LPS results in a higher blood concentration of IL-6 in α7-nAchR knockout (α7KO) mice than in controls (Wang et al., 2003). It has also been pointed out that the inflammation control mechanism of the vagus nerve serves an important role as a feedback mechanism in the inflammatory response, thereby preventing the excessive production of cytokines (Tracey, 2002). However, the role of the vagal control of Kupffer cells in physiological inter-organ communication between the CNS and liver has yet to be elucidated.

In this study, we found that the vagal Kupffer cell-suppressing action plays an important role in the central insulin action-mediated hepatic responses of IL-6/STAT3 signal activation and regulation of gluconeogenic enzyme gene expression. Central insulin action activates hepatic IL-6/STAT3 signaling by suppressing the activity of the hepatic branches of the vagus nerve and alleviating the vagal suppression of Kupffer cells. Moreover, we found that α7-nAchR is essential for central insulin action-mediated hepatic responses, as these responses were severely impeded in α7KO mice.

RESULTS

Central Insulin Action Suppresses Hepatic Vagal Activation, Inhibiting Hepatic IL-6/STAT3 Signaling

To investigate the regulation of vagus nerve activation by central insulin action, electrophysiological activity of the hepatic branches of the vagus nerve was measured under ICV insulin. Vagal nerve activity (VNA) of the hepatic branches diminished significantly in the ICV insulin group from 30 min after administration (Figure 1A). Therefore, we performed a hepatic branch vagotomy study to investigate the effect of diminished VNA on hepatic IL-6/STAT3. Vagotomy enhanced STAT3 phosphorylation and IL-6 expression in the liver (Figures 1B, S1A, and S1C). It is known that intravenous administration of liposome-encapsulated clodronate enables the removal of Kupffer cells, which are the major source of IL-6 in the liver (Kimura et al., 2013; Van Rooijen and Sanders, 1996), and indeed, in the present study, liposome-encapsulated clodronate treatment reduced the expression of the Kupffer cell and macrophage markers Emr1 and IL-6 in the liver, but not in adipose tissue or the spleen (Figures 1C and S1B). Immunohistochemical analysis using an anti-MAC2 antibody, which is used widely for the detection of monocytes/macrophages/Kupffer cells, also revealed the marked decrease of MAC2-positive cells in the liver following liposome-encapsulated clodronate treatment (Figure S1C). Following the reduction of hepatic IL-6 expression by the administration of liposome-encapsulated clodronate, vagotomy-induced hepatic STAT3 phosphorylation was diminished (Figures 1B, S1A, and S1C). Hepatic branch vagotomy resulted

(B and C) Wild-type (WT) mice were vagotomized or sham-operated and then treated with liposome-encapsulated clodronate. The STAT3 phosphorylation levels were determined at 4 days after vagotomy by western blotting (B), and the gene expression levels of Emr1 and IL-6 (C) were measured by qRT-PCR (*$p < 0.05$) (n = 8).

(D and E) Time-course changes in STAT3 phosphorylation and hepatic *Il6* mRNA after vagotomy. The liver was harvested at the indicated time, the STAT3 phosphorylation levels were determined by western blotting (D, lysates were pooled for each group), and the gene expression levels of IL-6 (E) were measured by qRT-PCR (*$p < 0.05$) (n = 6–10).

(F) Time-course change in STAT3 phosphorylation after chlorisondamine administration. The mice were administered chlorisondamine (0.25 mg/kg) intraperitoneally. The liver was harvested at the indicated time, and the STAT3 phosphorylation levels were determined by western blotting (lysates were pooled for each group). The quantitation of STAT3 phosphorylation levels is normalized to total STAT3 (right) (*$p < 0.05$) (n = 6).

(G and H) The mice were pre-treated with liposome-encapsulated clodronate and then given chlorisondamine (0.25 mg/kg) intraperitoneally. The liver was harvested at 4 hr after administration, and the STAT3 phosphorylation levels were determined by western blotting and quantitative densitometry. (G) Gene expression levels of IL-6 and Emr1 (H) were measured by qRT-PCR (*$p < 0.05$) (n = 6) (chlorisondamine, chlori; liposome-encapsulated clodronate, CLD; hepatic VNA, HVNA; insulin, Ins; vehicle, Veh; and vagotomy, Vx).

See also Figure S1.

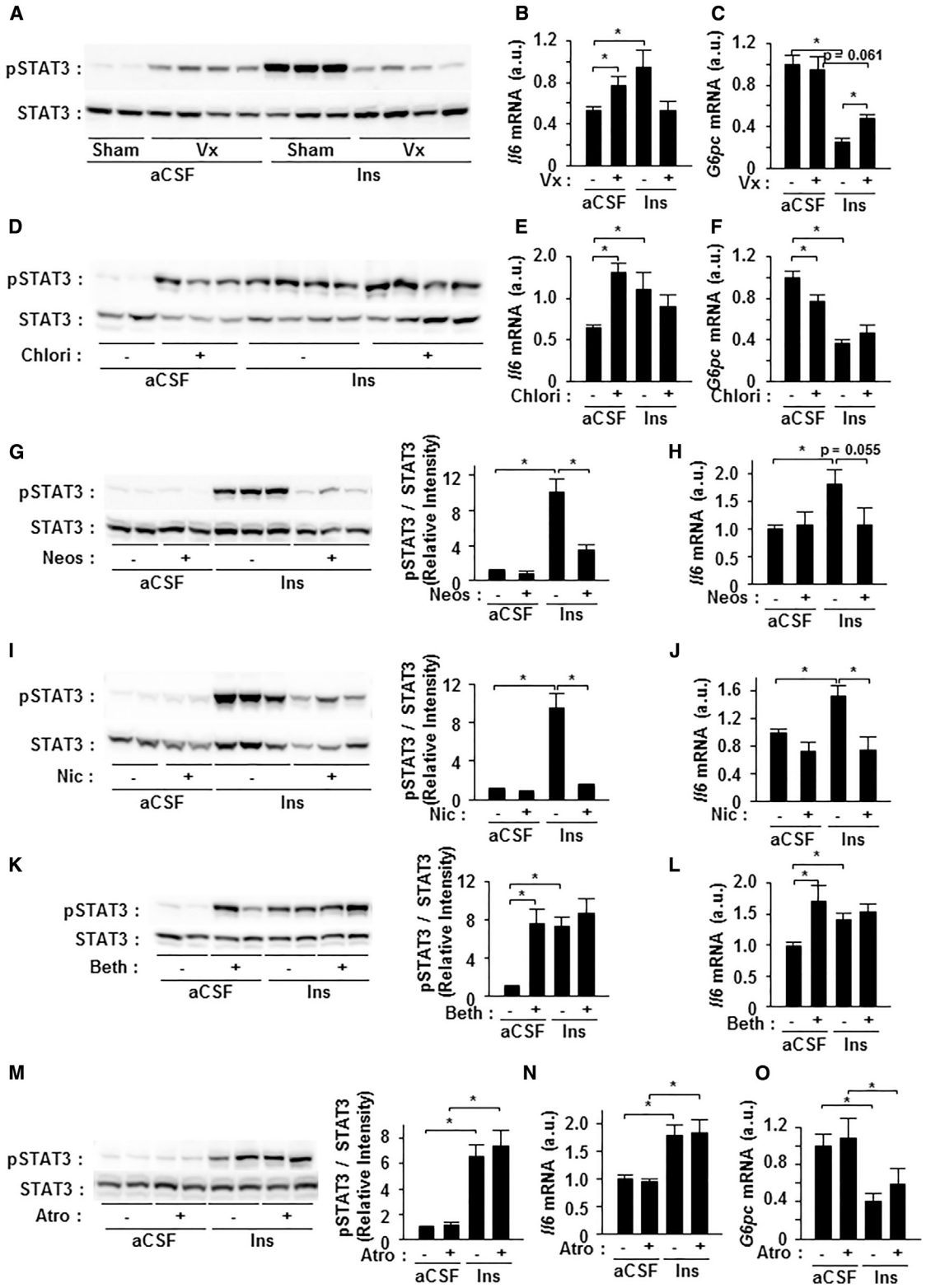

(legend on next page)

in enhanced hepatic STAT3 phosphorylation from 12 hr after excision, as well as a significant increase in hepatic IL-6 gene expression from 24 hr after excision (Figures 1D, S1D, and S1E). The surgical procedure, which induced acute and transient hepatic STAT3 phosphorylation in a vagotomy-independent manner, as shown by its phosphorylation until 12 hr after laparotomy in sham surgery groups (Figures 1D and S1D), prevented us from assessing the acute effects of vagal inactivation on hepatic IL-6/STAT3 activation. Therefore, we performed an investigation using chlorisondamine, which is a α7-nAchR antagonist, to evaluate the effect of acute blockage of vagal nicotinic cholinergic action on hepatic IL-6/STAT3. At low doses, chlorisondamine mainly blocks the effects of peripheral α7-nAchR, similar to an autonomic ganglion blocker (Clarke, 1984; Clarke et al., 1994). Hepatic STAT3 was phosphorylated from 3 to 12 hr after peripheral nicotinic cholinergic blockade by low-dose chlorisondamine administration (Figure 1F), and the increase of hepatic STAT3 phosphorylation by chlorisondamine administration was attenuated following the administration of liposome-encapsulated clodronate (Figure 1G). Chlorisondamine administration also increased IL-6 gene expression in the liver; however, liposome-encapsulated clodronate administration greatly diminished hepatic IL-6 expression, along with that of Emr1 (Figure 1H). These results suggest that central insulin action suppresses vagus nerve activity and that the decline in its activity induces the increase of IL-6 expression in Kupffer cells and hepatic STAT3 phosphorylation.

Vagal Blockade Abolishes Central Insulin-Mediated Regulation of Hepatic IL-6/ STAT3 Signaling and Gluconeogenic Gene Expression

ICV insulin induced STAT3 phosphorylation and IL-6 gene expression in the liver and suppressed the gene expression of G6Pase, a hepatic gluconeogenic enzyme (Figures 2A and S2A–S2C). Therefore, the role of the vagus nerve in central insulin action-mediated hepatic responses was investigated by vagotomy and chlorisondamine administration. At 4 days after vagotomy, STAT3 phosphorylation and IL-6 expression were slightly increased in the liver, but the hepatic IL-6/STAT3 signal activation response to ICV insulin administration was lost (Figures 2A, S2A, and S2B). In keeping with previous reports (Pocai et al., 2005b), vagotomy inhibited the ICV insulin-induced suppression of G6Pase gene expression (Figure 2C). Chlorisondamine administration increased hepatic STAT3 phosphorylation (Figures 2D and S2B), increased IL-6 gene expression (Figure 2E), and decreased G6Pase gene expression (Figure 2F). Yet, no additive effects were observed on hepatic responses by central insulin action under chlorisondamine administration, such as increased hepatic STAT3 phosphorylation and IL-6 gene expression or suppressed G6Pase expression (Figures 2D, S2B, S2E, and S2F). These results suggest that the vagus nerve suppresses IL-6/STAT3 signaling in the liver, and by inhibiting this suppression by the vagus nerve, central insulin action induces hepatic effects such as IL-6/STAT3 signal activation and the suppression of G6Pase gene expression.

The role of acetylcholine, which is the major neurotransmitter in the vagus nerve, in ICV insulin-induced hepatic IL-6/STAT3 activation was investigated. Amplification of its cholinergic effect via administration of the acetylcholinesterase inhibitor neostigmine diminished the ICV insulin-induced phosphorylation of hepatic STAT3 (Figure 2G). The ICV insulin-induced increase of IL-6 gene expression did not occur under neostigmine administration (Figure 2H). Moreover, central insulin action-mediated activation of hepatic IL-6/STAT3 signaling was inhibited by the administration of nicotine (Figures 2I and 2J). These results indicate that central insulin action may control IL-6 gene expression in Kupffer cells and STAT3 activation in hepatocytes via nicotinic cholinergic action. While the enhanced cholinergic action following neostigmine reduced hepatic STAT3 phosphorylation, administration of the muscarinic acetylcholine receptor agonist bethanechol increased hepatic IL-6 expression and STAT3 phosphorylation (Figures 2K and 2L). The muscarinic acetylcholine receptor antagonist, atropine, inhibited bethanecol-induced hepatic STAT3 activation (Figure S2C), but had no effect on ICV insulin-induced hepatic STAT3 phosphorylation, IL-6 increase, or G6pc decrease (Figures 2M–2O).

α7 Nicotinic Cholinergic Action Suppresses Kupffer Cell Activation

We investigated the suppressing effect of nicotinic cholinergic activity on IL-6 expression in isolated Kupffer cells. Acetylcholine reduced the LPS-dependent induction of IL-6 expression in isolated Kupffer cells (Figure 3A). Moreover, the LPS-dependent induction of IL-6 expression was suppressed in a dose-dependent manner with nicotine pre-treatment, but not with bethanechol pre-treatment (Figure 3B). Nicotine suppressed IL-6 expression, but this suppression was mitigated by chlorisondamine (Figure 3C). Next, we performed an investigation using α-bungarotoxin

Figure 2. Vagal Blockade Abolishes Central-Insulin Mediated Regulation of Hepatic IL-6/STAT3 Signaling and Gluconeogenic Gene Expression

(A–C) ICV insulin administration was performed at 4–6 days after vagotomy. The WT mice were given ICV insulin (10 μU/hr). The liver was harvested at 3 hr after administration, and the STAT3 phosphorylation levels were determined by western blotting (A). The gene expression levels of IL-6 (B) and G6Pase (C) were measured by qRT-PCR (*$p < 0.05$) (n = 11).

(D–F) Chlorisondamine (0.25 mg/kg) was injected intraperitoneally at 1 hr before insulin (10 μU/hr, ICV). The liver was harvested at 3 hr after insulin administration, and the STAT3 phosphorylation levels were determined by western blotting (D). The expression levels of IL-6 (E) and G6Pase (F) mRNA were measured by qRT-PCR (*$p < 0.05$) (n = 12).

(G–O) Neostigmine (G and H; 0.02 mg/kg), nicotine (I and J; 0.2 mg/kg), bethanechol (K and L; 3 mg/kg), and atropine (M and N; 0.1 mg/kg) were injected intraperitoneally at 15 min before insulin (10 μU/hr, ICV). The liver was harvested at 3 hr after administration, and the STAT3 phosphorylation levels were determined by western blotting and quantitative densitometry (G, I, K, and M). The gene expression levels of IL-6 (H, J, L, and N) and G6pc (O) were measured by qRT-PCR (*$p < 0.05$) (G and H, n = 9; I and J, n = 15; K and L, n = 10; and M–O, n = 6) (atropine, Atro; bethanechol, Beth; chlorisondamine, Chlori; insulin, Ins; neostigmine, Neos; nicotine, Nic; sham vagotomy, Sham; and vagotomy, Vx).

See also Figure S2.

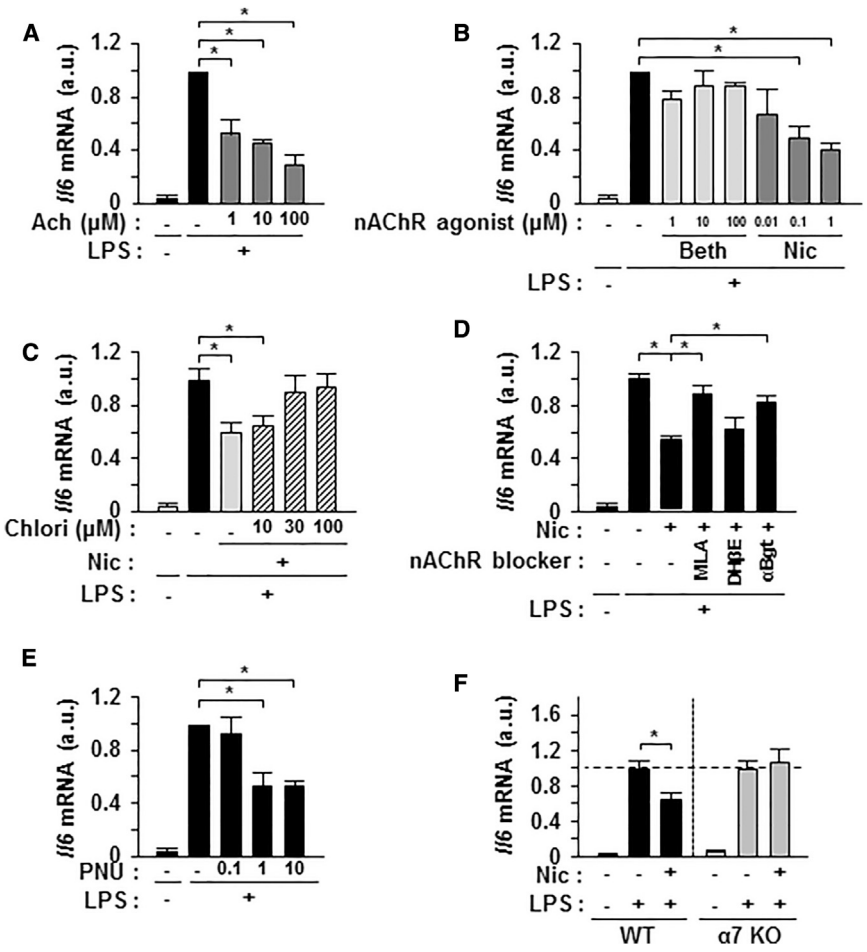

Figure 3. α7 Nicotinic Cholinergic Action Suppresses Kupffer Cell Activation

(A and B) Isolated Kupffer cell *Il6* mRNA levels stimulated by LPS after 15 min pre-treatment with acetylcholine (1, 10, and 100 μM with 1 mM pyridostigmine) (A), or with bethanechol (1, 10, and 100 μM), or nicotine (0.01, 0.1, and 1 μM) (B) (*$p < 0.05$) ($n = 4–6$).

(C and D) Gene expression levels of IL-6 in isolated Kupffer cells after LPS stimulation with 15 min pre-treatment of chlorisondamine (10, 30, and 100 μM) and/or nicotine (0.1 μM) (C) and with 15 min pre-treatment with MLA (1 μM) or DHβE (1 μM, 15 min) or αBgt (100 nM) and/or nicotine (0.1 μM) (D) (*$p < 0.05$) ($n = 6$).

(E) Isolated Kupffer cells were stimulated with LPS following 15 min pre-treatment with PNU-282987 (PNU; 0.1, 1, and 10 μM). The gene expression of IL-6 in Kupffer cells was measured by qRT-PCR (*$p < 0.05$) ($n = 6$).

(F) In WT or α7KO mouse-derived Kupffer cells, *Il6* mRNA levels were measured after LPS stimulation with 15 min of nicotine pre-treatment (0.1 μM; *$p < 0.05$; $n = 13$). α-Bgt; acetylcholine, Ach; bethanechol, Beth; chlorisondamine, Chlori; DhβE; and nicotine, Nic.

(αBgt), an inhibitor of the α1, α7, and α8 α7-nAchR subtypes; methyllycaconitine (MLA), an antagonist of the α7 receptor subtype (α7-nAchR); dihydro-β-erythroidine (DHβE), an antagonist of the α4β2 receptor, the predominant nAchR in the CNS (Holladay et al., 1997); and PNU-282987, an agonist of α7-nAchR (Bodnar et al., 2005; Holladay et al., 1997). The nicotine treatment-induced suppression of IL-6 expression was mitigated by αBgt and MLA, but DHβE had no effect (Figure 3D). The LPS-dependent induction of IL-6 expression was suppressed in a dose-dependent manner by PNU-282987 (Figure 3E). Moreover, the suppressive effect of nicotine on the LPS-dependent induction of IL-6 expression was lost in Kupffer cells isolated from α7KO mice (Figures 3F and S3A). These results suggest that acetylcholine suppressed IL-6 expression in Kupffer cells via α7-nAchR.

Ablation of α7 Cholinergic Action Impedes Hepatic Regulation of IL-6/STAT3 Activation and Gluconeogenic Gene Expression Induced by Central Insulin Action

The importance of α7-nAchR in the central insulin action-mediated hepatic response was investigated using PNU-282987 and MLA. Central insulin action-mediated hepatic IL-6/STAT3 activation was lost when PNU-282987 was administered (Figures 4A and 4B). Meanwhile, MLA administration enhanced IL-6 expression and STAT3 activation in the liver, but did not further increase the central insulin action-mediated upregulation of hepatic IL-6/STAT3 signal activation (Figures 4C and 4D). α7KO mice reportedly display glucose intolerance and insulin resistance following high-fat diet feeding (Wang et al., 2011). However, when kept on a standard diet, there was no significant difference between α7KO mice and controls in terms of body weight and blood glucose levels under *ad libitum* feeding or in their blood glucose and plasma insulin levels during a glucose tolerance test (Figures S3A–S3F). Genetic ablation of α7-nAchR increased hepatic STAT3 phosphorylation similarly to acute inhibition by MLA administration, though STAT3 phosphorylation in α7KO mice was milder than that following MLA administration (Figure 4E). Additionally, when ICV insulin was administered, α7KO mice displayed suppression of vagus nerve activity similar to wild-type mice, but the increase of hepatic IL-6 expression and STAT3 activation was diminished (Figures 4E–4G). Furthermore, the suppression of G6Pase expression caused by ICV insulin was impeded in α7KO mice compared with controls (Figure 4H). These results suggest that α7-nAchR contributes significantly to the central insulin action-mediated activation of hepatic IL-6/STAT3 signaling and suppression of G6Pase gene expression.

Reconstitution of Kupffer Cells with Wild-type Bone Marrow-Derived Cells Restores the Central Insulin-Induced Activation of Hepatic Responses in α7KO Mice

α7-nAchR is expressed in the CNS, autonomic ganglia, and macrophages (Holladay et al., 1997; Wang et al., 2003). To investigate

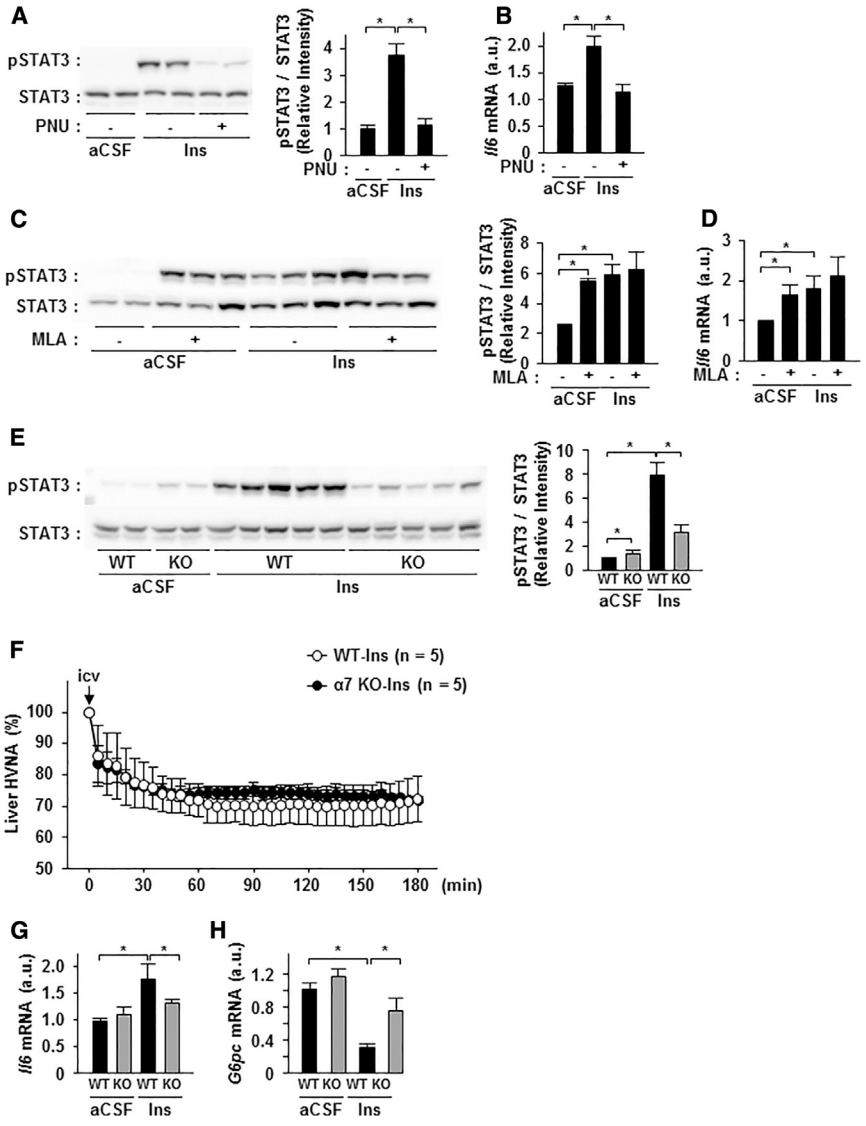

Figure 4. Ablation of α7 Cholinergic Action Attenuates IL-6/STAT3 Activation and Gluconeogenic Suppression Induced by Central Insulin Action

(A and B) STAT3 phosphorylation (A) and *Il6* mRNA (B) in the liver were measured at 3 hr after ICV insulin administration with 15 min subcutaneous pre-treatment of PNU (20 mg/kg; *p < 0.05; n = 9).

(C and D) STAT3 phosphorylation (C) and *Il6* mRNA (D) in the liver were measured at 3 hr after ICV insulin administration with 15 min intraperitoneal pre-treatment of MLA (0.1 mg/kg; *p < 0.05; n = 8).

(E, G, and H) STAT3 phosphorylation (E), *Il6* mRNA (G), and *G6pc* (H) mRNA in the liver of WT mice or α7KO mice were measured at 3 hr after ICV insulin administration. (E) Quantitation of STAT3 phosphorylation levels is normalized to total STAT3 (right; *p < 0.05; n = 13).

(F) Effects of insulin injection on hepatic VNA in mice. The time-course changes in hepatic VNA after ICV insulin injection to WT or α7KO mice are expressed as mean ± SEM of the percentages of values at 0 min. The open circles are ICV insulin injection to WT mice (n = 5), and the closed circles are ICV insulin injection to α7KO mice (n = 5). Hepatic VNA, HVNA and insulin, Ins.

See also Figure S3.

the importance of Kupffer cell α7-nAchR in central insulin action-mediated hepatic responses, we performed Kupffer cell replacement by bone marrow transplantation, and then tested the hepatic response to ICV insulin. Bone marrow transplantation with liposome-encapsulated clodronate treatment enables the reconstitution of Kupffer cells in recipient mice, in addition to hematopoietic cells, with those of donor mice (Seki et al., 2009). After bone marrow transplantation from eGFP transgenic mice to α7KO mice, 91.4% ± 3.3% (n = 3) of Kupffer cells in recipient α7KO mice were replaced with eGFP-positive Kupffer cells (Figure 5A) and α7-nAchR expression recovered in Kupffer cells isolated from recipient α7KO mice (Figure 5B). Replacement of α7KO Kupffer cells with their wild-type counterparts by transplanting wild-type mouse-derived bone marrow resulted in the recovery of the ICV insulin-induced hepatic responses of hepatic IL-6/STAT3 activation and G6Pase decrease (Figures 5C–5E).

To assess the role of Kupffer cell α7-nAchR in central insulin-mediated HGP regulation, we measured endogenous glucose production (EGP) in mice that underwent bone marrow transplantation, by a combination of ICV insulin infusion with pancreatic-insulin clamp studies (Figure 6A), as described previously (Inoue et al., 2006; Obici et al., 2002). In the protocol, plasma insulin levels were set to 0.466 ± 0.091 ng/ml (n = 6) in wild-type mice at 120 min after the start of intravenous insulin infusion. There was no significant difference in blood glucose levels between wild-type mice with wild-type bone marrow, α7KO mice with α7KO bone marrow, and α7KO mice with wild-type bone marrow at the basal state 240 min after the start of ICV insulin infusion and the clamp state between 90 and 120 min after starting intravenous insulin (Figures 6B and 6C). α7KO mice with α7KO bone marrow had a lower glucose infusion rate with impeded ICV insulin-induced suppression of EGP than wild-type mice with wild-type bone marrow transplantation, with no significant difference in the rate of disappearance (Figures 6D–6F). Reconstitution of wild-type Kupffer cells in α7KO mice by bone marrow transplantation restored the central insulin-mediated suppression of EGP (Figure 6F). These findings indicate that Kupffer cell α7-nAchR plays a significant role in the central insulin-mediated regulation of HGP.

Central Insulin-Mediated Vagal Suppression Is Blocked in Obese Insulin-Resistant Mice

Central insulin action-mediated metabolic control is impeded in obesity and insulin resistance (Ono et al., 2008; Spanswick et al.,

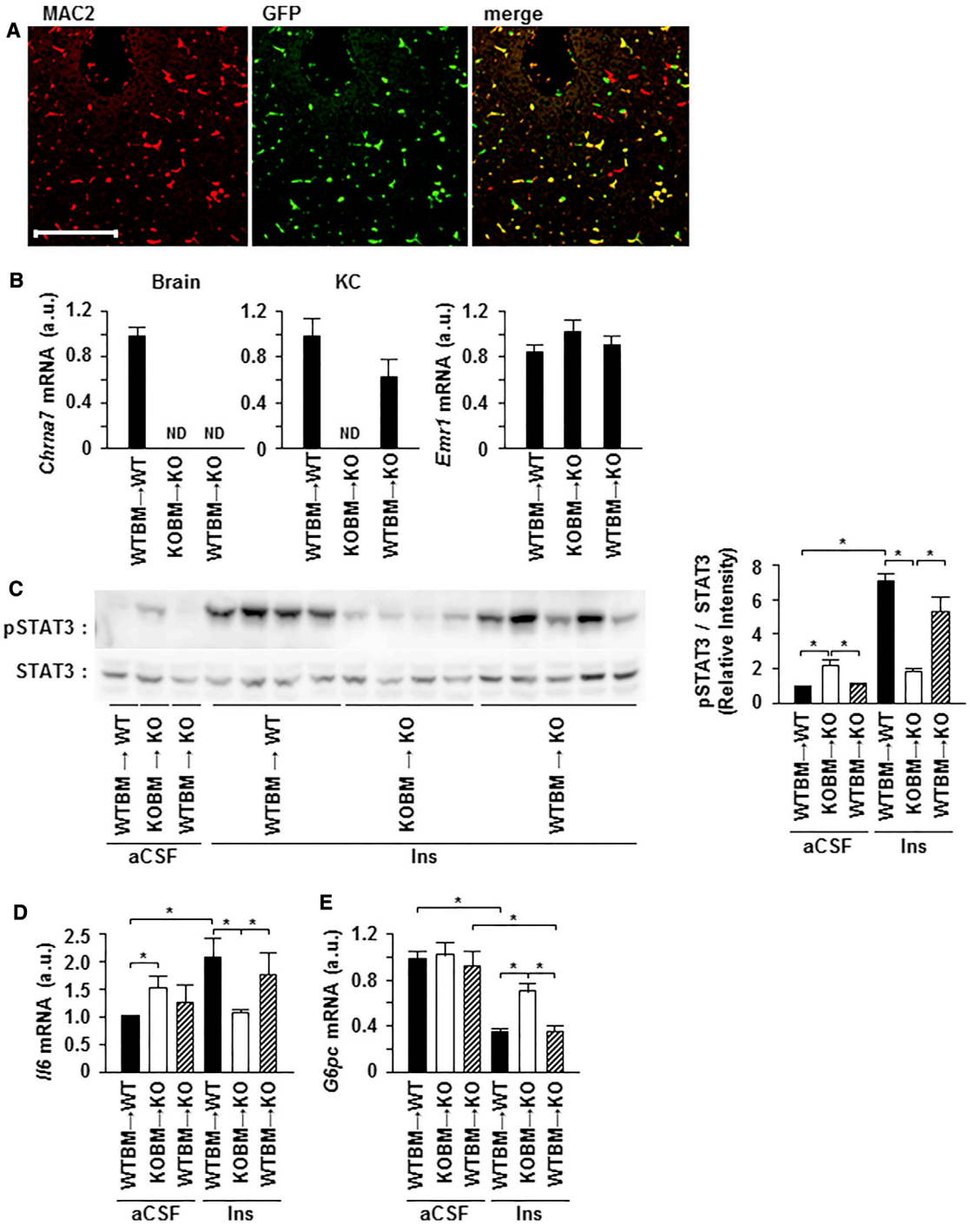

Figure 5. Reconstitution of WT Kupffer Cells in α7KO Mice Restores Central Insulin-Induced Hepatic IL-6/STAT3 Activation

(A) Hepatic Kupffer cells were analyzed by immunostaining using anti-MAC2 and anti-GFP antibodies in α7KO mice transplanted with GFP-transgenic mice-derived bone marrow. The scale bar represents 100 mm.

(B) Gene expression of α7-nAchR in brain and Kupffer cells and of Emr1 in the liver of WT mice with WT bone marrow transplantation (BMT) (n = 6), α7KO mice with α7KO-BMT (n = 7), or WT-BMT mice (n = 6).

(C–E) STAT3 phosphorylation (C), *Il6* mRNA (D), and *G6pc* mRNA (E) levels in mice with Kupffer cell reconstitution after ICV insulin administration (*p < 0.05; n = 6–10).

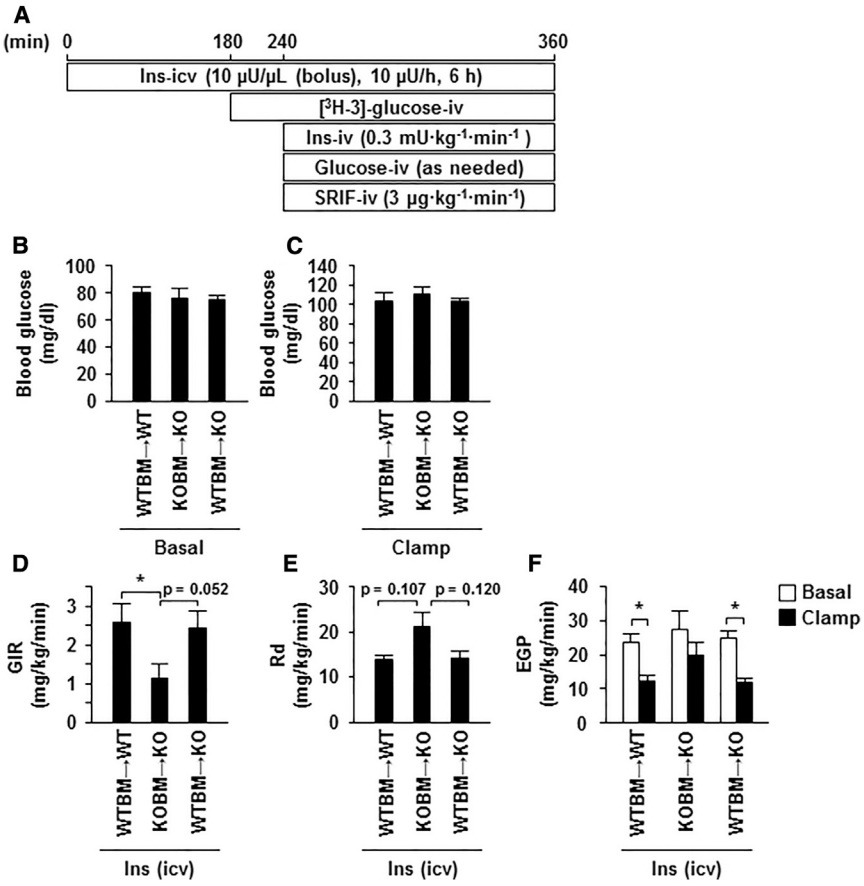

Figure 6. Reconstitution of WT Kupffer Cells Restores Central Insulin-Mediated Suppression of EGP in α7KO Mice

(A) A euglycemic pancreatic-insulin clamp with ICV insulin infusion was performed as shown in the schematic.

(B–F) Blood glucose levels before (B) and during the last 30 min of the euglycemic clamp tests (C), glucose infusion rate (GIR) (D), rate of disappearance (Rd) (E), and EGP before and after intravenous insulin infusion (F) (*$p < 0.05$; $n = 6$).

2000). Indeed, ICV insulin does not lead to a change in vagus nerve activity, and the suppression of G6Pase gene expression is impeded (Figures 7A and 7B) in mice displaying obesity and hyperinsulinemia after receiving a high-fat diet for 6 weeks (Figures S4A–S4C). Hepatic expression of IL-6 was amplified in mice with high-fat diet feeding, but the increased expression of IL-6 normally induced by ICV insulin was lost (Figure 7B). Chlorisondamine administration resulted in increased hepatic expression of IL-6 in lean mice due to the acute alleviation of the vagal suppression of Kupffer cells, but resulted in no change in high-fat diet-induced obese mice (Figure 7C). Meanwhile, PNU administration lowered the increased expression of IL-6 in the liver of high-fat diet mice (Figure 7D), suggesting that a cholinergic effect leads to Kupffer cell suppression even in diet-induced obese mice. Together, these results suggest that central insulin action-mediated vagus nerve control is lost, and that the suppression of IL-6 expression in Kupffer cells by the vagus nerve is impeded in obese insulin-resistant mice.

DISCUSSION

Autonomic nerve-mediated crosstalk between the CNS and peripheral organs serves an important function in the maintenance of glucose/energy metabolism homeostasis by insulin. In particular, the importance of the vagus nerve in the central insulin action-mediated suppression of HGP has been indicated by previous studies of hepatic vagotomy (Pocai et al., 2005b). In a previous report, we showed that central insulin action suppresses the gene transcription of hepatic gluconeogenic enzymes via the activation of hepatic IL-6/STAT3 signaling, that is, increased IL-6 expression in Kupffer cells and activation of hepatocyte STAT3 (Inoue et al., 2006). The induction of hepatic IL-6/STAT3 signaling activation by central insulin action has been confirmed in dogs as well as in rodents, suggesting the interspecies conservation of the mechanism of the central insulin action-mediated hepatic response (Ramnanan et al., 2011). However, the molecular mechanism by which central insulin action elicits hepatic responses via the vagus nerve has not yet been elucidated. In this study, we showed that central insulin suppresses vagus nerve activity, resulting in hepatic IL-6/STAT3 activation and HGP decrease via α7-nAchR. A recent paper suggested that the activity of the vagus nerve is suppressed by activation of the melanocortin 4 receptor, a receptor of α-melanocyte-stimulating hormone (α-MSH) (Sohn et al., 2013), and it has been also reported that central administration of α-MSH decreases HGP (Obici et al., 2001). These findings may be related to our present finding that the suppression of vagus nerve activity results in decreased HGP, though it has been indicated that central insulin action suppresses HGP in an α-MSH-independent manner (Obici et al., 2002).

Insulin action in hypothalamic agouti-related peptide (AgRP) neurons reportedly has a significant role in central insulin-mediated HGP suppression. In AgRP neuron-specific insulin receptor KO mice, the insulin-dependent suppression of HGP is impeded during euglycemic hyperinsulinemic clamp studies (Könner et al., 2007). The insulin-mediated decrease of HGP is not impeded in proopiomelanocortin (POMC) neuron-specific insulin receptor KO mice (Könner et al., 2007), but is impaired in POMC neuron-specific leptin receptor/insulin receptor double KO mice (Hill et al., 2010), possibly indicating the importance of hypothalamic POMC neurons. We revealed that ICV insulin suppressed the activity of the hepatic branches of the vagal nerve, but elucidation of a vagus nerve regulation mechanism by insulin in the CNS remains a future challenge.

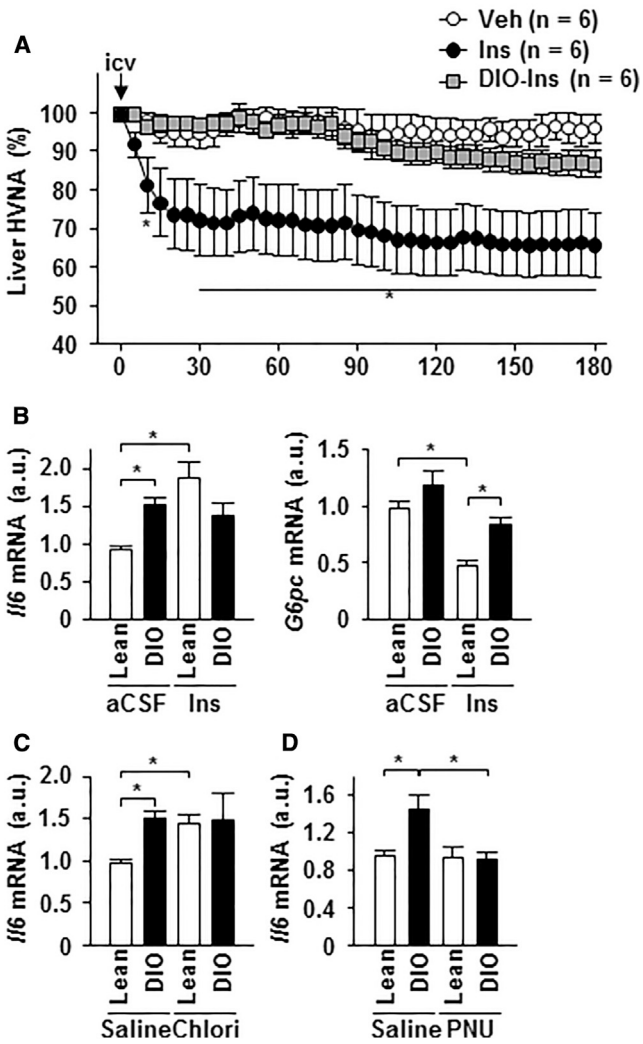

Figure 7. Central Insulin-Mediated Vagal Suppression Is Blocked in Obese Insulin-Resistant Mice

(A) Hepatic VNA in diet-induced obesity (DIO) insulin-resistant mice after ICV insulin infusion. The data are expressed as mean ± SE of the percentages of values at 0 min. The open circles are ICV-aCSF bolus injection to lean mice (n = 6). The closed circles are ICV insulin injection to lean mice (n = 6). The gray squares are ICV insulin injection to DIO mice (n = 6).

(B) Gene expression levels of IL-6 and G6Pase in lean and DIO mice with ICV insulin (*$p < 0.05$; n = 14).

(C and D) Gene expression levels of IL-6 in lean and DIO mice at 4 hr after intraperitoneal administration of chlorisondamine (0.25 mg/kg; C; n = 9) or at 3 hr after subcutaneous administration of PNU (20 mg/kg; D; n = 11–13; *$p < 0.05$). Insulin, Ins; hepatic VNA, HVNA; and vehicle, Veh.

See also Figure S4.

The acute shutdown of vagal cholinergic activity by the administration of the α7-nAchR antagonist chlorisondamine resulted in increased hepatic IL-6 expression and STAT3 phosphorylation. Meanwhile, the administration of liposome-encapsulated clodronate, which depletes Kupffer cells in the liver, but not macrophages in adipose tissue, abrogated both the hepatic increase of IL-6 expression and STAT3 phosphorylation induced by chlorisondamine administration. These findings indicate that suppression of vagal action can increase IL-6 expression in Kupffer cells, which induces hepatic STAT3 phosphorylation. As a previous study reported that STAT3 phosphorylation appears for a brief period and declines thereafter by persistent stimulation of IL-6 (Lang et al., 2003), the cellular responses to IL-6 are different between chronic persistent and acute stimulation of IL-6 (Awazawa et al., 2011). Indeed, chronic inhibition of vagus nerve activity by vagotomy leads to a persistent increase of IL-6 expression, but a much milder enhancement of hepatic STAT3 phosphorylation, at more than 24 hr after vagotomy, which would not be sufficient to decrease G6Pase expression. The increase of IL-6 expression in Kupffer cells by suppression of vagus nerve activity may decay with time, whereas the ablation of the vagal control of Kupffer cells persists. Indeed, hepatic IL-6/STAT3 signaling was activated as potently by the acute inhibition of α7-nAchR by MLA as by chlorisondamine administration, while the chronic disruption of α7-nAchR in α7KO mice revealed no significant increase in hepatic IL-6 expression and much milder activation of hepatic STAT3 as compared with chronic vagal inhibition by vagotomy. In fact, α7-nAchR deficiency resulted in no difference of G6Pase expression in the fasting state compared with controls. ICV insulin attenuated vagus nerve activity, followed by hepatic IL-6/STAT3 activation. However, with vagal blockage, namely via chlorisondamine administration or vagotomy, the ICV insulin-mediated boost of hepatic IL-6/STAT3 signaling activation was inhibited. These results suggest that the suppressive action of the vagus nerve on IL-6 expression in Kupffer cells plays an important role in central insulin action-mediated hepatic responses. Meanwhile, vagotomy failed to increase hepatic IL-6/STAT3 activation under the condition of ICV insulin, which may suggest the existence of a central insulin action-mediated counter regulatory mechanism that suppresses hepatic IL-6/STAT3 signaling.

The central insulin action-mediated hepatic response of IL-6/STAT3 activation amplification was lost with the administration of chlorisondamine or MLA and suppressed with the administration of nicotine and PNU-282987. In α7KO mice, the ICV insulin-induced hepatic activation of STAT3 and suppressed expression of G6Pase were impeded. These findings suggest that vagal α7-nAchR action plays an important role in central insulin action-mediated hepatic responses. The vagus nerve forms synapses with post-synaptic fibers at the intrahepatic autonomic ganglia. α7-nAchR is also expressed in the ganglia, as in Kupffer cells (McCuskey, 2004; Uyama et al., 2004). In primary cultures of Kupffer cells, LPS-dependent inflammatory cytokine expression was suppressed by the action of α7-nAchR. Additionally, replacement of Kupffer cells in α7KO mice with wild-type counterparts led to the recovery of ICV insulin-induced IL-6/STAT3 activation and HGP suppression. These observations are indicative of the importance of Kupffer cell α7-nAchR in central insulin action-mediated hepatic responses. In contrast, the role of muscarinic cholinergic action in centrally mediated hepatic responses remains to be elucidated. The muscarinic acetylcholine receptor antagonist, atropine, had no effect on the ICV insulin-induced increase of IL-6 expression and STAT3 phosphorylation in the liver at the dose at which bethanecol-induced hepatic STAT3 phosphorylation was inhibited. However, the enhanced cholinergic action following neostigmine

administration potently decreased hepatic IL-6/STAT3 activation; conversely, the enhanced muscarinic cholinergic action following bethanechol administration increased hepatic IL-6/STAT3 activation, though bethanechol treatment had little influence on the LPS-induced expression of IL-6 in isolated Kupffer cells. These findings may indicate that muscarinic cholinergic action acts as a feedforward mechanism of nicotinic cholinergic action in centrally medicated hepatic responses.

Obesity and insulin resistance impair central insulin action in the hypothalamus (Ono et al., 2008; Spanswick et al., 2000). Indeed, our investigation showed that ICV insulin failed to elicit changes in vagus nerve activity of high-fat diet-induced obese mice. Hepatic IL-6 expression was suppressed by PNU-282987 administration in high-fat diet-induced obese mice, suggesting that cholinergic action suppresses IL-6 expression even in obese and insulin-resistant mice. However, hepatic IL-6 expression was not amplified by acute blockade of vagal cholinergic action by chlorisondamine administration in high-fat diet-induced obese mice, indicating that the vagal control of suppressing IL-6 expression in hepatic Kupffer cells was disrupted in obese mice in the same manner as in hepatic vagotomy. In obesity-induced insulin resistance, metabolites and humoral factors, including free fatty acids and tumor necrosis factor, lead to chronic inflammation in the liver, which exacerbates hepatic insulin resistance (Gregor and Hotamisligil, 2011). Although α7-nAchR deficiency did not enhance hepatic IL-6 expression, possibly due to prolonged ablation of the vagal control of Kupffer cells, the inflammation-induced increases of hepatic inflammatory cytokines are reportedly upregulated in α7KO mice (Wang et al., 2003). In addition to these proinflammatory stimuli, such as metabolites and humoral factors resulting from obesity and insulin resistance, it is plausible that the impairment of central insulin-mediated vagal action via α7-nAchR that suppresses hepatic inflammatory cytokine expression contributes to chronic hepatic inflammation. In obesity and insulin-resistance, hepatic IL-6 increase failed to reduce G6Pase gene expression. As shown in our vagotomy experiments, the persistent increase of IL-6 expression revealed much milder activation of hepatic STAT3 than the acute increase of IL-6 induced by acute blockade of cholinergic action. Furthermore, it has been reported that a low-grade proinflammatory state in obese mice results in a mild increase in the basal activation and blunting of the acute activation response of hepatic STAT3 by IL-6 (Gruber et al., 2013; Kimura et al., 2012), which would be insufficient to suppress HGP in spite of the persistent increase of IL-6 expression in obese and insulin-resistant mice.

In this study, we have elucidated the mechanism by which the vagus nerve suppresses hepatic IL-6/STAT3 signaling activation via Kupffer cell α7-nAchR-mediated cholinergic activity, as well as the mechanism by which central insulin action amplifies hepatic IL-6/STAT3 activity by lowering the activity of the hepatic branches of the vagus nerve. Moreover, we found the possibility that central insulin action-mediated control of the vagus nerve is lost, while cholinergic action has the ability to suppress inflammatory cytokine expression in Kupffer cells in obese insulin-resistant mice. These findings suggest that the aberrant regulation of Kupffer cells via the vagus nerve and α7-nAchR-mediated cholinergic action by central insulin action may have a significant role in the pathogenesis of chronic hepatic inflammation in obesity.

EXPERIMENTAL PROCEDURES

Mice

Experiments using mice were conducted in accordance with the guidelines for the care and use of laboratory animals of Kanazawa University. Male mice (8–10 weeks old) were housed under a 12 hr light-dark cycle with free access to food and water. Wild-type C57BL/6J Slc mice were purchased from Japan SLC, and α7KO mice were from Jackson Laboratory. Diet-induced obesity mice were fed a high-fat diet (60% fat, D12492; Research Diets) for 4 or 6 weeks from 7 weeks of age.

Electro-Physiological Recording of Hepatic VNA

Parasympathetic nerve activity measurements were performed as described previously (Tanida et al., 2015). In brief, the hepatic branch of the ventral subdiaphragmatic vagal nerve was identified and exposed on the esophagus after incision of the abdominal midline, to measure hepatic VNA. Hepatic VNA was recorded in separate animals. Each nerve was attached to a pair of 36-gauge stainless steel wire electrodes and then fixed quickly with a silicone gel (Kwik-Sil; WPI) to prevent dehydration and provide electrical insulation. After surgery, each animal was allowed to stabilize for 20–40 min.

Electrical activity in each nerve was amplified 50,000–100,000 times with a band-pass filter of 100–1,000 kHz and monitored using an oscilloscope. The amplified and filtered nerve activity was converted to standard pulses by a window discriminator, which separated discharges from electrical background noise post-mortem. Both the discharge rates and the neurogram were sampled with a PowerLab analog-to-digital converter for recording and data analysis on a computer. Background noise, which was determined at 30–60 min after the animal was euthanized, was subtracted. Nerve activity was rectified and integrated with baseline nerve activity normalized to 100%.

Baseline measurements of hepatic VNA were made at 5–10 min prior to ICV bolus injection of vehicle (artificial cerebrospinal fluid 2 μl) and human insulin (40 μU/2 μl). After treatment, nerve activity was monitored for 180 min. At the end of the experiment, hexamethonium bromide (10 mg/kg body weight) was administered intravenously to ensure that post-ganglionic efferent parasympathetic nerve activity had been recorded.

ICV Administration of Insulin

An internal cannula (Plastics One) was inserted into the lateral ventricle. After 7–10 days of recovery and then a 16 hr fast, the mice received an ICV administration of human insulin or artificial cerebrospinal fluid (Inoue et al., 2006). An insulin (10 μU/μl) solution was infused at a fixed rate (1 μl/hr) following bolus infusion (1 μl/min). The mice received chlorisondamine, neostigmine, nicotine, bethanechol, atropine, PNU-282987, and MLA (Sigma-Aldrich) with ICV insulin administration, as described in the figure legends.

Euglycemic Pancreatic-Insulin Clamp Procedure

A euglycemic pancreatic-insulin clamp test was carried out as described previously with modifications (Kimura et al., 2013). An internal cannula (Plastics One) was inserted into the lateral ventricle, followed by intravenous cannulation at 7–9 days later. After 4 days of recovery and habituation, we performed pancreatic clamp with ICV administration. After a 16 hr fast, the mice received an ICV administration of porcine insulin (Sigma-Aldrich) with an intravenous injection of [3H]glucose (Perkin Elmer), glucose, human insulin (Eli Lilly), and somatostatin (SRIF), as shown in Figure 6A. Blood glucose levels were measured every 10 min and maintained between 90 and 120 mg/dl after starting intravenous injections of insulin and SRIF. Between 90 and 120 min after starting insulin and SRIF administration, the glucose infusion rate and plasma [3H] glucose-specific activity was measured every 10 min. The rate of disappearance (Rd) under steady-state conditions for plasma glucose concentration was determined from the rate of [3H]glucose infusion divided by plasma [3H] glucose-specific activity. The rate of EGP was obtained from the difference between Rd and glucose infusion rate.

Kupffer Cell Depletion or Reconstitution by Bone Marrow Transplantation

Kupffer cell depletion was performed as described previously (Kimura et al., 2013). For Kupffer cell reconstitution by bone marrow transplantation, we injected liposomal clodronate (Clophosome; FormuMax Scientific) intravenously at 2 and 3 days before irradiation to deplete Kupffer cells (Seki et al., 2009). Bone marrow was obtained by flushing the tibias and femurs of donor mice and then washing twice in ice-cold PBS containing 0.5% BSA. Bone marrow transplantation was performed by injecting 1.0×10^8 bone marrow cells into the tail veins of irradiated (4.8 Gy, twice) recipient mice. The ICV insulin injection study was performed at 6 weeks after bone marrow transplantation. The efficacy of Kupffer cell reconstitution was evaluated by immunostaining with an anti-mouse MAC2 antibody (Cedarlane Laboratories) and anti-GFP antibody (Medical and Biological Laboratories) in α7KO liver transplanted from GFP-transgenic mice (Okabe et al., 1997).

Identification, Isolation, and Culture of Kupffer Cells

Kupffer cell counting was performed for the analysis of immunohistochemistry using an anti-MAC2 antibody (Cedarlane Laboratories). Kupffer cells were isolated as described previously, with minor modifications (Ikeda et al., 2009). In brief, the liver was perfused through the vena cava with Krebs-Ringer buffer containing calcium and magnesium ions. Thereafter, the liver was minced and incubated in a buffer containing 0.1% type 1 collagenase (Worthington Biochemical) and 150 U/ml DNase for 30 min. The suspension was filtered through a 100-μm filter membrane and the filtrate was centrifuged twice at 50 × *g* for 4 min at 4°C to remove parenchymal cells. The remaining cell fraction in the supernatant was resuspended in Dulbecco's modified Eagle medium (DMEM) containing 10% heat-inactivated fetal calf serum and allowed to adhere to the bottom of plastic culture dishes for 3 hr. Non-adherent cells were removed by gentle washing. LPS (Sigma-Aldrich) was added to the culture medium at a final concentration of 5 ng/ml, and the cells were collected at 3 hr after stimulation with LPS. The cells were pre-treated with the following agents for 15 min prior to LPS administration: acetylcholine with pyridostigmine, bethanechol, nicotine, chlorisondamine, PNU-282987, MLA (Sigma-Aldrich), DHβE (Tocris Bioscience), and αBgt (Tocris Bioscience).

Analysis of Blood Parameters

Plasma insulin and IL-6 concentration was determined using a mouse insulin ELISA kit (Shibayagi) and Quantikine Mouse IL-6 ELISA kit (R&D Systems), respectively. Blood glucose levels were measured using a GLUCOCARD G+ Meter (Arkray). Serum endotoxin concentrations were quantified by a limulus amoebocyte lysate (LAL kit, QCL-1000; Lonza). Sterile serum samples obtained from portal vein blood were diluted to 20% (vol/vol) with endotoxin-free water and heated to 70°C for 10 min to inactivate serum proteins. Each assay was performed strictly according to the manufacturers' protocols.

Western Blotting and qPCR

Immunoblotting was performed using an anti-phosphorylated (phospho)-STAT3 (Tyr705) antibody (Cell Signaling Technology) and anti-STAT3 antibody (Santa Cruz Biotechnology). Immunoblot images are representative of at least three independent immunoblot analyses and quantified by densitometry on an LAS-3000 Imager (Fujifilm).

The results of qPCR were analyzed using the 36B4 gene as an internal control and plotted in arbitrary units as mean ± SE. The primer sequences used in this study are available upon request (*36B4*, *Il6*, *Emr1*, *Chrna7* [which encodes α7-nAchR], and *G6pc* [which encodes G6Pase]).

Statistical Analysis

Data are represented as mean ± SE. Statistical analysis was performed using Student's t test and one-way ANOVA followed by post hoc tests and differences were considered significant at p values of < 0.05.

SUPPLEMENTAL INFORMATION

Supplemental Information includes four figures and can be found with this article online at http://dx.doi.org/10.1016/j.celrep.2016.02.032.

AUTHOR CONTRIBUTIONS

K.K. and M.T. produced the data and contributed to the discussion. N.N., Y.I., H.W., M.N., S.A., and K.T. produced the data. T.O., Y.K., M.M., M.N., T.S., S.K., and M.K. contributed to the discussion and reviewed and edited the manuscript. H.I. researched the data, designed the study, contributed to the discussion, wrote the manuscript, and is the guarantor.

CONFLICTS OF INTEREST

The authors report no conflict of interest regarding this publication.

ACKNOWLEDGMENTS

We thank K. Nagamori, M. Nishio, and C. Asahi, Kanazawa University for providing technical assistance; H. Nakabayashi, Kanazawa University for providing a technique for hepatic vagotomy, and ThinkSCIENCE (Tokyo, Japan) for help preparing the manuscript. This work was supported by the Japan Society for the Promotion of Science KAKENHI grants 15H01373, 26282022, and 26670599 to H.I. and 26860693 to K.K.

Received: July 21, 2015
Revised: November 23, 2015
Accepted: February 1, 2016
Published: March 3, 2016

REFERENCES

Akira, S. (1997). IL-6-regulated transcription factors. Int. J. Biochem. Cell Biol. *29*, 1401–1418.

Awazawa, M., Ueki, K., Inabe, K., Yamauchi, T., Kubota, N., Kaneko, K., Kobayashi, M., Iwane, A., Sasako, T., Okazaki, Y., et al. (2011). Adiponectin enhances insulin sensitivity by increasing hepatic IRS-2 expression via a macrophage-derived IL-6-dependent pathway. Cell Metab. *13*, 401–412.

Bodnar, A.L., Cortes-Burgos, L.A., Cook, K.K., Dinh, D.M., Groppi, V.E., Hajos, M., Higdon, N.R., Hoffmann, W.E., Hurst, R.S., Myers, J.K., et al. (2005). Discovery and structure-activity relationship of quinuclidine benzamides as agonists of alpha7 nicotinic acetylcholine receptors. J. Med. Chem. *48*, 905–908.

Borovikova, L.V., Ivanova, S., Zhang, M., Yang, H., Botchkina, G.I., Watkins, L.R., Wang, H., Abumrad, N., Eaton, J.W., and Tracey, K.J. (2000). Vagus nerve stimulation attenuates the systemic inflammatory response to endotoxin. Nature *405*, 458–462.

Brüning, J.C., Gautam, D., Burks, D.J., Gillette, J., Schubert, M., Orban, P.C., Klein, R., Krone, W., Müller-Wieland, D., and Kahn, C.R. (2000). Role of brain insulin receptor in control of body weight and reproduction. Science *289*, 2122–2125.

Carey, M., Kehlenbrink, S., and Hawkins, M. (2013). Evidence for central regulation of glucose metabolism. J. Biol. Chem. *288*, 34981–34988.

Clarke, P.B. (1984). Chronic central nicotinic blockade after a single administration of the bisquaternary ganglion-blocking drug chlorisondamine. Br. J. Pharmacol. *83*, 527–535.

Clarke, P.B., Chaudieu, I., el-Bizri, H., Boksa, P., Quik, M., Esplin, B.A., and Capek, R. (1994). The pharmacology of the nicotinic antagonist, chlorisondamine, investigated in rat brain and autonomic ganglion. Br. J. Pharmacol. *111*, 397–405.

Gregor, M.F., and Hotamisligil, G.S. (2011). Inflammatory mechanisms in obesity. Annu. Rev. Immunol. *29*, 415–445.

Gruber, S., Straub, B.K., Ackermann, P.J., Wunderlich, C.M., Mauer, J., Seeger, J.M., Büning, H., Heukamp, L., Kashkar, H., Schirmacher, P., et al. (2013). Obesity promotes liver carcinogenesis via Mcl-1 stabilization independent of IL-6Rα signaling. Cell Rep. *4*, 669–680.

Hill, J.W., Elias, C.F., Fukuda, M., Williams, K.W., Berglund, E.D., Holland, W.L., Cho, Y.R., Chuang, J.C., Xu, Y., Choi, M., et al. (2010). Direct insulin and leptin action on pro-opiomelanocortin neurons is required for normal glucose homeostasis and fertility. Cell Metab. *11*, 286–297.

Holladay, M.W., Dart, M.J., and Lynch, J.K. (1997). Neuronal nicotinic acetylcholine receptors as targets for drug discovery. J. Med. Chem. *40*, 4169–4194.

Ikeda, O., Ozaki, M., Murata, S., Matsuo, R., Nakano, Y., Watanabe, M., Hisakura, K., Myronovych, A., Kawasaki, T., Kohno, K., and Ohkohchi, N. (2009). Autonomic regulation of liver regeneration after partial hepatectomy in mice. J. Surg. Res. *152*, 218–223.

Inoue, H., Ogawa, W., Ozaki, M., Haga, S., Matsumoto, M., Furukawa, K., Hashimoto, N., Kido, Y., Mori, T., Sakaue, H., et al. (2004). Role of STAT-3 in regulation of hepatic gluconeogenic genes and carbohydrate metabolism in vivo. Nat. Med. *10*, 168–174.

Inoue, H., Ogawa, W., Asakawa, A., Okamoto, Y., Nishizawa, A., Matsumoto, M., Teshigawara, K., Matsuki, Y., Watanabe, E., Hiramatsu, R., et al. (2006). Role of hepatic STAT3 in brain-insulin action on hepatic glucose production. Cell Metab. *3*, 267–275.

Kimura, K., Yamada, T., Matsumoto, M., Kido, Y., Hosooka, T., Asahara, S., Matsuda, T., Ota, T., Watanabe, H., Sai, Y., et al. (2012). Endoplasmic reticulum stress inhibits STAT3-dependent suppression of hepatic gluconeogenesis via dephosphorylation and deacetylation. Diabetes *61*, 61–73.

Kimura, K., Nakamura, Y., Inaba, Y., Matsumoto, M., Kido, Y., Asahara, S., Matsuda, T., Watanabe, H., Maeda, A., Inagaki, F., et al. (2013). Histidine augments the suppression of hepatic glucose production by central insulin action. Diabetes *62*, 2266–2277.

Könner, A.C., Janoschek, R., Plum, L., Jordan, S.D., Rother, E., Ma, X., Xu, C., Enriori, P., Hampel, B., Barsh, G.S., et al. (2007). Insulin action in AgRP-expressing neurons is required for suppression of hepatic glucose production. Cell Metab. *5*, 438–449.

Lang, R., Pauleau, A.L., Parganas, E., Takahashi, Y., Mages, J., Ihle, J.N., Rutschman, R., and Murray, P.J. (2003). SOCS3 regulates the plasticity of gp130 signaling. Nat. Immunol. *4*, 546–550.

McCuskey, R.S. (2004). Anatomy of efferent hepatic nerves. Anat. Rec. A Discov. Mol. Cell. Evol. Biol. *280*, 821–826.

Obici, S., Feng, Z., Tan, J., Liu, L., Karkanias, G., and Rossetti, L. (2001). Central melanocortin receptors regulate insulin action. J. Clin. Invest. *108*, 1079–1085.

Obici, S., Zhang, B.B., Karkanias, G., and Rossetti, L. (2002). Hypothalamic insulin signaling is required for inhibition of glucose production. Nat. Med. *8*, 1376–1382.

Okabe, M., Ikawa, M., Kominami, K., Nakanishi, T., and Nishimune, Y. (1997). 'Green mice' as a source of ubiquitous green cells. FEBS Lett. *407*, 313–319.

Ono, H., Pocai, A., Wang, Y., Sakoda, H., Asano, T., Backer, J.M., Schwartz, G.J., and Rossetti, L. (2008). Activation of hypothalamic S6 kinase mediates diet-induced hepatic insulin resistance in rats. J. Clin. Invest. *118*, 2959–2968.

Plum, L., Belgardt, B.F., and Brüning, J.C. (2006). Central insulin action in energy and glucose homeostasis. J. Clin. Invest. *116*, 1761–1766.

Pocai, A., Lam, T.K., Gutierrez-Juarez, R., Obici, S., Schwartz, G.J., Bryan, J., Aguilar-Bryan, L., and Rossetti, L. (2005a). Hypothalamic K(ATP) channels control hepatic glucose production. Nature *434*, 1026–1031.

Pocai, A., Obici, S., Schwartz, G.J., and Rossetti, L. (2005b). A brain-liver circuit regulates glucose homeostasis. Cell Metab. *1*, 53–61.

Prodi, E., and Obici, S. (2006). Minireview: the brain as a molecular target for diabetic therapy. Endocrinology *147*, 2664–2669.

Ramadoss, P., Unger-Smith, N.E., Lam, F.S., and Hollenberg, A.N. (2009). STAT3 targets the regulatory regions of gluconeogenic genes in vivo. Mol. Endocrinol. *23*, 827–837.

Ramnanan, C.J., Saraswathi, V., Smith, M.S., Donahue, E.P., Farmer, B., Farmer, T.D., Neal, D., Williams, P.E., Lautz, M., Mari, A., et al. (2011). Brain insulin action augments hepatic glycogen synthesis without suppressing glucose production or gluconeogenesis in dogs. J. Clin. Invest. *121*, 3713–3723.

Schwartz, M.W., Seeley, R.J., Tschöp, M.H., Woods, S.C., Morton, G.J., Myers, M.G., and D'Alessio, D. (2013). Cooperation between brain and islet in glucose homeostasis and diabetes. Nature *503*, 59–66.

Seki, E., de Minicis, S., Inokuchi, S., Taura, K., Miyai, K., van Rooijen, N., Schwabe, R.F., and Brenner, D.A. (2009). CCR2 promotes hepatic fibrosis in mice. Hepatology *50*, 185–197.

Sohn, J.W., Harris, L.E., Berglund, E.D., Liu, T., Vong, L., Lowell, B.B., Balthasar, N., Williams, K.W., and Elmquist, J.K. (2013). Melanocortin 4 receptors reciprocally regulate sympathetic and parasympathetic preganglionic neurons. Cell *152*, 612–619.

Spanswick, D., Smith, M.A., Mirshamsi, S., Routh, V.H., and Ashford, M.L. (2000). Insulin activates ATP-sensitive K+ channels in hypothalamic neurons of lean, but not obese rats. Nat. Neurosci. *3*, 757–758.

Tanida, M., Yamamoto, N., Morgan, D.A., Kurata, Y., Shibamoto, T., and Rahmouni, K. (2015). Leptin receptor signaling in the hypothalamus regulates hepatic autonomic nerve activity via phosphatidylinositol 3-kinase and AMP-activated protein kinase. J. Neurosci. *35*, 474–484.

Tracey, K.J. (2002). The inflammatory reflex. Nature *420*, 853–859.

Uyama, N., Geerts, A., and Reynaert, H. (2004). Neural connections between the hypothalamus and the liver. Anat. Rec. A Disc. Mol. Cell. Evol. Biol. *280*, 808–820.

Van Rooijen, N., and Sanders, A. (1996). Kupffer cell depletion by liposome-delivered drugs: comparative activity of intracellular clodronate, propamidine, and ethylenediaminetetraacetic acid. Hepatology *23*, 1239–1243.

Wang, H., Yu, M., Ochani, M., Amella, C.A., Tanovic, M., Susarla, S., Li, J.H., Wang, H., Yang, H., Ulloa, L., et al. (2003). Nicotinic acetylcholine receptor alpha7 subunit is an essential regulator of inflammation. Nature *421*, 384–388.

Wang, X., Yang, Z., Xue, B., and Shi, H. (2011). Activation of the cholinergic antiinflammatory pathway ameliorates obesity-induced inflammation and insulin resistance. Endocrinology *152*, 836–846.